

## Submitted version on Author's Personal Website: C. R. Koch

Article Name with DOI link to Final Published Version complete citation:

M. Shahbakhti, R. Lupul, and C. R. Koch. Predicting HCCI auto-ignition timing by extending a modified knock-integral method. In *SAE Paper 2007-01-0222*, April 2007

### See also:

[https://sites.ualberta.ca/~ckoch/open\\_access/Shahbakhti2007.pdf](https://sites.ualberta.ca/~ckoch/open_access/Shahbakhti2007.pdf)

Pre-print

As per publisher copyright is ©2007



This work is licensed under a [Creative Commons Attribution-NonCommercial-NoDerivatives 4.0 International License](https://creativecommons.org/licenses/by-nc-nd/4.0/).



Article submitted version starts on the next page →

[Or link: to Author's Website](#)

# Predicting HCCI Auto-Ignition Timing by Extending a Modified Knock-Integral Method

Mahdi Shahbakhti, Robert Lupul, Charles Robert Koch  
University of Alberta, Canada

Copyright © 2007 Society of Automotive Engineers, Inc.

## ABSTRACT

One major challenge in Homogeneous Charge Compression Ignition (HCCI) combustion is the difficulty in controlling the timing of auto-ignition which is dependant on mixture conditions. Understanding the effect of modifying the properties of the engine charge on the start of combustion is essential to be able to predict and control the auto-ignition timing. The purpose of this work is to develop a realtime model for predicting HCCI auto-ignition timing.

The standard Livengood and Wu Knock-Integral Method (KIM) is modified to work with values that are easier to measure compared with the instantaneous in-cylinder parameters required in the original KIM. This modified Knock-Integral Method (MKIM) is developed and is then parameterized using HCCI Thermokinetic Kinetic Model (TKM) simulations for a single cylinder engine. Estimating the MKIM parameters is done using an off-line optimization technique. Once the parameters have been identified, the MKIM needs only the rate of Exhaust Gas Recirculated (EGR), equivalence ratio, intake manifold temperature and intake manifold pressure to predict auto-ignition timing. The MKIM is validated with the experimental data from the single cylinder engine in HCCI operation by varying equivalence ratio, EGR level, engine speed, and intake temperature for three different blends of Primary Reference Fuels (PRF) at octane values of 0, 10 and 20.

## INTRODUCTION

A promising method for reducing emissions and fuel consumption of internal combustion engines is the HCCI engine that incorporates the best features of both the SI (Spark Ignition) and the diesel engines [1, 2]. HCCI engines can significantly reduce NO<sub>x</sub> and particulate emissions, while achieving high thermal efficiency and the ca-

pability of operating with a wide variety of fuels. There are a number of obstacles that must be overcome before the potential benefits of HCCI combustion can be fully realized in production applications. HCCI combustion has three main difficulties including: Control of combustion timing, Limited power output, and Homogenous mixture preparation [2]. Controlling the timing of auto-ignition is the most serious problem [3]. This is because the HCCI engine lacks features for direct control of the combustion timing. In an HCCI engine, once the initial conditions are set, it is difficult to affect the combustion timing. Precise control of temperature, pressure and composition of the air fuel mixture is needed to prevent misfires, excessive peak pressure and excessive pressure gradient, all of which can damage the engine and increase NO<sub>x</sub> generation. Simulation models of HCCI combustion timing can be used to accurately schedule cylinder charge properties for desired auto-ignition timing.

A variety of models has been used to simulate the auto-ignition timing of HCCI engines. They differ in the complexity and required input data. These models range from multi-dimensional CFD models [4, 5] and multi-zone models [6, 7], to simple control-oriented models [8, 9]. For real-time control, a compromise between the computation time and accuracy of the model is required. Low-order control oriented models can predict auto-ignition timing of HCCI engines with a reasonable accuracy while having short computational time [10]. Control oriented modeling of HCCI combustion is grouped into the following six categories of models. In the simplest approach, HCCI combustion timing is mapped into look-up tables as a function of the engine variables which have been experimentally found to predominantly affect HCCI combustion [11]. This requires a large number of experiments, and may not work outside the region the engine has been mapped. The second simplest model defines a temperature threshold to find the start of combustion [12]. The basis of this model

is that the mixture temperature has the most dominant effect on the reaction rate of reactions that control HCCI auto-ignition delay. This model fails to capture combustion phasing at different operating conditions, which is due to the dependence of the initiation of the combustion reaction on not only the temperature but also on the concentration of species present in the cylinder. The Shell model [13] is another model used in [8] to predict HCCI auto-ignition timing. The results from the Shell model show an accurate estimation of the HCCI auto-ignition timing for a temperature and engine speed sweep, but less accurate results when changing the load. In [8, 10, 14], models based on Arrhenius-type reaction rate [15] are used. Here the integration of the Arrhenius global reaction rate for the fuel is tracked until it reaches a threshold value defined from experimental data. To parameterize the model, the values of the constants are taken from tabulated values for hydrocarbons [15]. This model type is accurate, but depends on having instantaneous fuel and oxygen concentrations as well as in-cylinder gas temperature which is impractical for on-board control of auto-ignition timing.

To remove the need for in-cylinder composition data, some researches [16, 17] omitted the mixture composition term from the Arrhenius reaction rate. This simplified Arrhenius based model uses the idea that the composition term in Arrhenius reaction rate is in the secondary importance compared to other terms. Their results seem accurate in the studied HCCI range, but the model should be validated for a wide range of HCCI operation. The knock-integral model [18] is a fifth category in control-oriented modeling of HCCI combustion timing. This model is based on an exponential correlation which includes the elements of in-cylinder gas pressure and temperature to predict the auto-ignition of a homogeneous mixture [19, 20, 21]. Although this model produces accurate results, again there is a need for some parameters which are difficult and expensive to measure. This limits using this model for real-time control. To make more accurate and more practical models, a sixth category of models has been defined. Two examples from this category are the models in [22] and [23] in which the compression process is considered a polytropic process to remove model's requirement for instantaneous in-cylinder gas temperature and pressure. Other example includes the model presented in [24] where the effects of residual gas and air fuel ratio (AFR) have been added to the knock-integral model and also another model [21] in which a pressure term has been added to the knock-integral model to benefit from the physics of Arrhenius reaction rate based models.

Despite the extensive work done on control-oriented modeling of auto-ignition timing for HCCI engines, improved models that work with easily measurable inputs and which include variable working conditions are still needed. The model proposed in this paper addresses some of the compromises of existing models. In particular, it is designed to be a control-oriented model which also works for different conditions including variable load, air temperature, engine speed, AFR, and EGR. Instantaneous in-cylinder

gas temperature, pressure or the concentrations of fuel and oxygen are not required, instead measured EGR rate, AFR and intake manifold temperature and pressure are required. This model improves our previous work [23] in that the intake temperature and pressure are used. Furthermore, the limited experimental validation done in our previous work for a constant intake temperature and constant engine speed condition is augmented by cross-validating of the model with new experimental data in which engine variables (intake temperature, EGR, equivalence ratio, intake pressure and engine speed) are varied<sup>1</sup>. To test the performance of the model for different engines, new validation is done on an engine, different from that of our previous work. It will be also shown that the model can predict not only the start of main HCCI combustion but also the start of the cool flame combustion.

In this study, three different blends of N-heptane and iso-octane are used as the fuel. This selection is done as N-heptane and iso-octane are primary reference fuels (PRFs) for octane rating in internal combustion engines, and have the cetane number of approximately 56 and 15, with octane numbers of 0 and 100, which is very similar to the cetane number of conventional diesel fuel and gasoline, respectively. Therefore, a better understanding of HCCI engines fueled with PRFs and their mixtures is useful to control HCCI auto-ignition timing [3]. The performance of the model is evaluated for three different PRF blends (PRF0, PRF10, PRF20)<sup>2</sup>

In this paper, the first section explains the model developed to predict HCCI auto-ignition timing and also the model to calculate the mixture condition at the Intake Valve Closing (IVC) moment. Then the methodology used to parameterize the model is shown and our existing HCCI Thermo-Kinetic Model (TKM) [25] is used as a virtual engine to produce the required data for parameter estimation of the model. Next, the experimental setup used in this study is explained and the conditions of the HCCI experiments are detailed. Then the proposed model is applied to HCCI combustion and the performance of the model is validated for experiments at different engine conditions. Finally, after discussing the results, conclusions are reached and future research tasks are outlined.

## MODEL DESCRIPTION

In this section, two correlations are introduced to relate the values of intake manifold pressure and temperature to their values at IVC crank angles. Then, the modifications of the original Knock Integral Model into a Modified Knock Integral Model are explained.

---

<sup>1</sup>Most of the control oriented HCCI ignition models have been validated over a narrow range of HCCI operation.

<sup>2</sup>PRF number is defined as the volume percentage of iso-octane in fuel mixture of N-heptane and iso-octane.

## IVC TEMPERATURE & PRESSURE CORRELATION

HCCI combustion is mainly affected by the properties of air fuel mixture at IVC instant when the closed part of the engine cycle begins. In production port fuel injection engines the temperature and pressure of the intake air mixture is usually measured in the intake manifold, with fuel injected downstream near the intake valve. While in an HCCI engine, intake temperature and pressure at IVC are needed to predict the start of combustion (SOC). Temperature and pressure of the air fuel mixture change from the intake manifold to the cylinder at IVC. This is mainly caused by heat transfer between the mixture and cylinder walls and also the gas dynamics during the gas exchange process. If the change of mixture temperature and pressure is ignored and their measured values in the intake manifold are used instead of their IVC values, the HCCI combustion code that works with those IVC values yields erroneous SOC. Here, two simple correlations are introduced to predict pressure and temperature of the mixture at IVC using their measured values in the intake manifold.

Table 1 shows how IVC gas pressure is expected to change when other parameters are changed within the HCCI operating range of the engine used in this study. The manifold gas pressure directly influences the gas pressure at IVC,  $P_{ivc}$ . When intake manifold temperature is increased or the equivalence ratio is decreased the mass of in-cylinder charge decrease, which that leads to a decrease in  $P_{ivc}$ . An increase in the engine speed results in less wall heat transfer which promotes an increase in  $P_{ivc}$ . EGR has a small influence on  $P_{ivc}$  that mainly comes from its dilution effect on changing the mass of in-cylinder charge.

Table 1: Expected trend of change in IVC gas pressure with other parameters

Parameter	$P_{ivc}$
Engine Speed, $N \uparrow$	$\uparrow$
EGR Fraction $\uparrow$	$\downarrow$
Equivalence Ratio, $\Phi \uparrow$	$\uparrow$
Manifold Pressure, $P_{man} \uparrow$	$\uparrow$
Manifold Temperature, $T_{man} \uparrow$	$\downarrow$

After trying different correlations based on the physics introduced in Table 1, the following correlation provided a good fit to the available experimental data (that will be introduced later in *Experimental Setup* section of the paper):

$$P_{ivc} = \frac{N^{0.038} \times \Phi^{0.020}}{T_{man}^{0.022}} \times P_{man} \quad (1)$$

where,  $N$  is in rpm and  $P_{man}$  in kiloPascals (kPa) and  $T_{man}$  in degrees Celsius (C). Equation (1) indicates that

the EGR influence can be neglected in the correlation and after  $P_{man}$ , engine speed has the most dominant influence on  $P_{ivc}$ , while  $\Phi$  and  $T_{man}$  are of lower importance respectively.

The correlation (1) has an average error and standard error of 1.33 kPa and 0.97 kPa respectively and the maximum relative error is less than 4%, when compared to the experimental data.

It is difficult to measure the mixture temperature at IVC,  $T_{ivc}$ . To get the values of  $T_{ivc}$ , the TKM<sup>3</sup> (HCCI combustion model) is run for the experimental HCCI points used in this study. The  $T_{ivc}$  that leads to a good agreement between the simulated and experimental SOC is chosen as the correct  $T_{ivc}$ . Examining the  $T_{ivc}$  values obtained, it was noticed that almost all of the HCCI combustions occur in a 25-degree window of  $T_{ivc}$  ( $100^\circ C \leq T_{ivc} \leq 125^\circ C$ ). Furthermore, by plotting the change of  $T_{ivc}$  with  $T_{man}$ , it was noticed that after a specific intake temperature (i.e.  $T_{man} = 110^\circ C$ ),  $T_{ivc}$  decreases with an increase in  $T_{man}$ , while the reverse trend is seen for the cases with  $T_{man}$  lower than  $110^\circ C$ . This comes from a change in the direction of heat transfer between the in-cylinder mixture and cylinder walls, where a constant wall temperature is assumed for the available HCCI experiments (all of which have been performed in fully warmed up condition).

After trying different possible correlations which have physical meaning, the following correlation was found to provide a good fit to the available experimental data:

$$T_{ivc} = (a \times T_{man} + b) \times \frac{\Phi^c \times N^d}{(1 + EGR)^e} \quad (2)$$

where  $a$ ,  $b$ ,  $c$ ,  $d$ , and  $e$  are the parameters of the correlation that are determined. Using a built-in Matlab function (*fminsearch*), these parameters are estimated. Table 2 shows the values of the estimated parameters in the correlation (2). The correlation suggests a linear relation between gas temperature at IVC and the intake manifold temperature. As seen in Table 2, the sign of  $a$  is changed from positive to negative when  $T_{man} < 110^\circ C$  compared to  $T_{man} \geq 110^\circ C$ . This indicates a change of heat transfer direction after a certain thermal condition. The correlation also suggests that  $T_{ivc}$  is increased with an increase in engine speed. This can be caused by a combination of effects of pressure rise in cylinder gas and the less available time for heat transfer. Furthermore, when  $T_{man} < 110^\circ C$ ,  $T_{ivc}$  is decreased with an increase in EGR, while it is increased with an increase in equivalence ratio. This trend is reversed when  $T_{man} \geq 110^\circ C$ . Since EGR and  $\Phi$  influence the amount of the heat transfer, but the direction of heat transfer is controlled by the temperature difference between the in-cylinder gas temperature and cylinder wall temperature. Increasing EGR leads to an increase in the

<sup>3</sup>The details of the TKM used is explained later in *Model Setup* section of the paper.

specific heat capacity of the mixture that reduces the rate of temperature change.

Table 2: Values of the parameters in  $T_{ivc}$  correlation - equation (2)

$T_{man} < 110^{\circ}\text{C}$			
Fuels	PRF0	PRF10	PRF20
a	0.68	0.474	0.694
b	121	180.8	285
c	0.096	0.134	0.185
d	-0.076	-0.084	-0.141
e	0.0033	0.0206	0.027
$110^{\circ}\text{C} \leq T_{man} \leq 140^{\circ}\text{C}$			
Fuels	PRF0	PRF10	PRF20
a	-0.0019	-0.369	–
b	110.3	450.5	–
c	-0.187	-0.029	–
d	-0.021	-0.191	–
e	-0.0146	-0.0153	–

Using the correlation (2) for the available experimental data, the maximum average error and maximum standard error are  $3.1^{\circ}\text{C}$  and  $2.9^{\circ}\text{C}$  respectively. Clearly this simple model, although useful for a real-time engine control algorithm, does not capture all of the physics of this complex process.

However, it should be noted that the IVC correlations introduced in this section have been tuned to experimental data from an engine with a constant valve timing at a fully warmed-up condition. How well this correlation will work for conditions where the gas exchange process is changed by cam timing or during thermal transients of heat transfer through cylinder walls (e.g. warm up condition) is unknown.

## AUTO-IGNITION TIMING MODEL

In this section, the definition of the auto-ignition point used in this study is explained. Then the original Knock Internal Model is briefly introduced and its extension into the Modified Knock Integral Model is explained.

### Auto-ignition Point Definition

All of the saturated compounds including paraffins such as N-heptane and iso-octane show two-stage combustion [26]. Two-stage combustion of N-heptane and iso-octane and their blends is associated with internal isomerization reactions in peroxy radicals [26]. The first combustion stage is controlled by low-temperature chemical reactions in particular by the fast reactions involving N-heptane. According to the low-temperature reaction mechanism, the first-stage combustion of hydrocarbon fuels is largely associated with ketohydroperoxide species decomposition

at a temperature between 800K and 850K, and the end of the first stage occurs when the temperature reaches the NTC<sup>4</sup> region. In the NTC region, temperature increases by slightly exothermic reactions that produce  $\text{H}_2\text{O}_2$ . The second stage combustion starts when the temperature approaches 1000K when the decomposition of  $\text{H}_2\text{O}_2$  becomes slower than its production [3]. By the second stage combustion, a pressure rise will occur that leads to a temperature rise, which added to the compression temperature results in an auto-ignition temperature for the explosive phase.

Either the cool flame combustion or the main combustion event can be used as the definition of SOC. In this study, SOC is defined as being the point at which the third derivative of the pressure trace with respect to the crank angle ( $\theta$ ) in CAD (Crank Angle Degree) exceeds a heuristically determined limit ( $\text{dp3Lim}$ ) [27]:

$$\left. \frac{d^3 P}{d\theta^3} \right|_{ign} = \left. \frac{d^3 P}{d\theta^3} \right|_{lim} \frac{\text{kPa}}{\text{CAD}^3} \quad (3)$$

To capture the beginning of the cool flame as the SOC,  $\text{dp3Lim } 5 \frac{\text{kPa}}{\text{CAD}^3}$  is used and to capture the main combustion as the SOC,  $\text{dp3Lim } 15 \frac{\text{kPa}}{\text{CAD}^3}$  is chosen. These two  $\text{dp3Lim}$  values are determined from the available experimental data that will be introduced later in the paper.

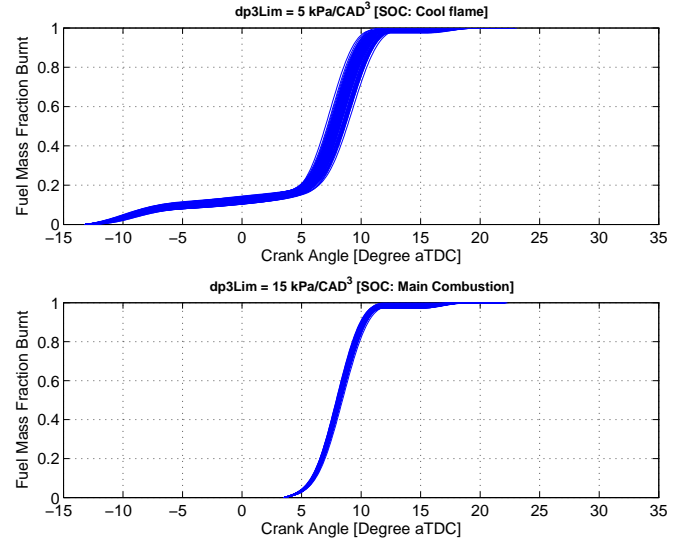


Figure 1: Mass fraction burnt curve for a sample experimental point, using two different  $\text{dp3Lim}$  values for 100 consecutive cycles.

Figure 1 shows the result of applying the two  $\text{dp3Lim}$  values for a sample experimental point. Fuel mass fraction burnt in Figure 1 has been determined by using Rassweiler method [28] on pressure traces from 100 consecutive cycles for the corresponding experimental point. As shown the cool flame is not captured when the higher

<sup>4</sup>Negative Temperature Coefficient region is a temperature zone in which the overall reaction rate decreases with increasing temperature.

value of  $dp3Lim$  is applied and instead the main combustion (2nd stage) is captured as the SOC.

### Knock Integral Model (KIM)

Kinetics of HCCI combustion are very similar to the chemical kinetics of knock in SI (Spark Ignition) engines [17]. Knock (premature auto-ignition) in SI engines has been investigated for decades [18, 29]. To predict the conditions under which knock would occur for various fuels was needed, Livengood and Wu [18] developed the first correlation to predict the autoignition of a homogeneous mixture, it was later termed the Knock-Integral Method (KIM) [30]. The basis of the correlation stems from the ignition delay of various fuels using a rapid compression testing machine. The resulting empirical relationship in the general form is:

$$\tau = Ae^{(b/T)p^n} \quad (4)$$

where  $\tau$  is the ignition delay,  $T$  is the mixture temperature as a function of time,  $p$  is the mixture pressure as a function of time, and  $A$ ,  $b$ , and  $n$  are empirical constants. The constants are the model parameters which are determined for each engine.

Livengood and Wu proposed that there is a functional relationship between the concentration ratio,  $(x)/(x)_c$ , of the significant species in the reaction and the relative time,  $t/\tau$ . The critical concentration ratio,  $(x)_c$ , is the concentration of the species at the end of the reaction being studied. Using the crank angle instead of time, the ignition correlation of Livengood and Wu becomes:

$$\frac{(x)}{(x)_c} = \int_{\theta_o=0}^{\theta=\theta_e} \frac{1}{\omega\tau} d\theta = \int_{\theta_o=0}^{\theta=\theta_e} \frac{1}{A\omega e^{(b/T)p^n}} d\theta = 1.0 \quad (5)$$

where  $\theta_e$  is the crank angle that autoignition or knock occurs and  $\theta_o$  is the initial crank angle where the integration begins. The engine speed ( $\omega$ ) is represented in revolutions per minute (rpm), the pressure in kiloPascals (kPa), and the temperature in Kelvin (K). The value of  $\theta_o$  is selected to be the crank angle of IVC timing where no appreciable reaction has begun ( $\theta_o = \theta_{IVC}$ ). The value of the expression being integrated ( $1/(\omega\tau)$ ) increases as the point of autoignition is approached as shown in Figure 2.

### Modified Knock-Integral Model (MKIM)

Although the KIM can predict HCCI auto-ignition, it is impractical for a real engine operation. Engine conditions, such as temperature, pressure and mass fraction burned, must be available during compression. In TKM simulations this is possible, but on a real engine, it is not. Furthermore, the KIM is for an engine operating at a constant AFR with no EGR. To adapt this correlation to a typical

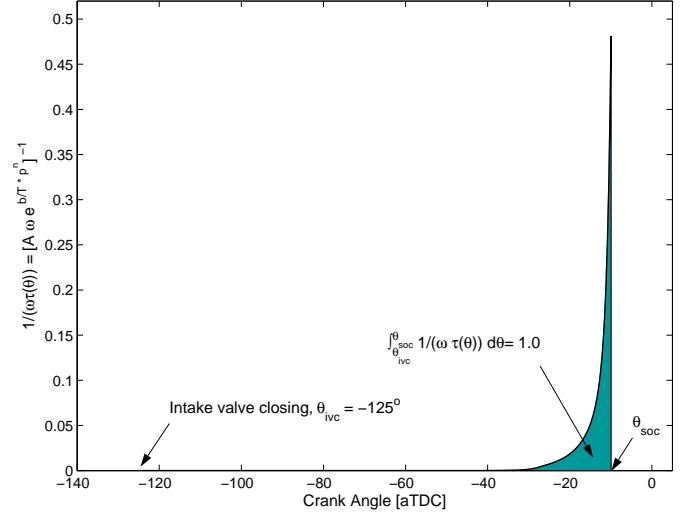


Figure 2: Graphical integration of  $1/(\omega\tau)$  from the intake valve closing to the start of combustion. In this example, the start of combustion is defined by equation (3) with  $dp3Lim = 5 \frac{kPa}{CAD^3}$ .

HCCI engine with varying AFR rates and EGR, these factors have to be accounted for.

The KIM is enhanced with these three modifications to address the problems mentioned above:

1. Polytropic compression. To avoid the requirement of crank angle measurements of temperature and pressure throughout the engine compression, the temperature and pressure rise in the cylinder is assumed to occur as a polytropic process [16]. Any pre-ignition heating that results from reactions that occur before the SOC is neglected.
2. Variable AFR. The SOC changes when the concentrations of the fuel and oxygen is varied [3, 26]. A crank angle measurement of these concentrations can be fed into a modified KIM to account for the AFR changes, but this information is only available in the TKM simulations and is not available in the real engine. An approach similar to that used to describe the polytropic process can be developed to predict the concentrations during compression. Therefore only the initial concentrations of the fuel and oxygen are required. But in most engine applications, the initial concentrations of the fuel and oxygen are not available. Although it is possible to determine these parameters using an exhaust gas analyzer and oxygen sensors, an exhaust analyzer is not present on production engines. Representing the initial concentrations of fuel and oxygen as the parameters that are easy to measure, but still describe the amount of fuel and air in the engine is more practical.

The equivalence ratio ( $\phi$ ) is a measure of the concentrations of the fuel and oxygen [8, 12] and it can

be measured on an operating engine without difficulty using a broadband oxygen sensor. Therefore, an equivalence ratio ( $\phi$ ) term is added to the KIM to account for the changes in AFR of the mixture.

3. Variable EGR. For some fuels such as iso-octane the amount of EGR changes the ability of the correlation to accurately predict the auto-ignition point. To generalize the correlation for all fuels, one term is added to account for the changes in EGR levels.

The resulting MKIM is [23]:

$$\int_{\theta_{IVC}}^{\theta_{SOC}} \frac{\phi^x}{A \omega \exp\left(\frac{b(P_{IVC} v_c^{n_c})^n}{T_{IVC} v_c^{n_c-1}}\right)} d\theta = 1.0 \quad (6)$$

$$\text{where } v_c(\theta) = \frac{V(\theta_{IVC})}{V(\theta)}, \quad A = C_1 EGR + C_2$$

where,  $C_1$ ,  $C_2$ ,  $b$ ,  $n$ ,  $n_c$ , and  $x$  are constant parameters. The constant  $n_c$  represents the average specific heat capacity ratio of all the simulations determined by a numeric best fit. The volume of the cylinder is calculated at any crank angle from engine geometry.

## MODEL SETUP

Figure 3 shows the overall methodology used in this study to parameterize and validate the MKIM. To parameterize the MKIM, three steps are required. First, simulation data covering a diverse range of the engine operation is collected and this data is used as the estimation data to parameterize the MKIM. Second, the polytropic parameter ( $n_c$ ) is determined using a best-fit methodology over the compression part of the simulation data. Third, an optimization is used to find the best values for the parameters of the MKIM. These three steps are detailed below.

### THERMOKINETIC MODEL SIMULATIONS

For accurate parameter estimation, the MKIM requires a large amount of the data from the engine at different working conditions. Due to cost limitations and potential hazard of damaging the engine by intense knocking when running the engine at the extreme operating points, it may not be possible to run the engine for a large number of experiments over a wide range of conditions. TKM is used as a virtual engine to provide the required data to parameterize the MKIM.

The TKM used is a single zone thermo-kinetic model modified from [25] to describe the in-cylinder thermo-kinetic state of an HCCI engine from intake valve closing to exhaust valve opening. The chemical kinetic mechanism, consisting of 58 species and 102 reactions, is used to describe the combustion of arbitrary primary reference fuel

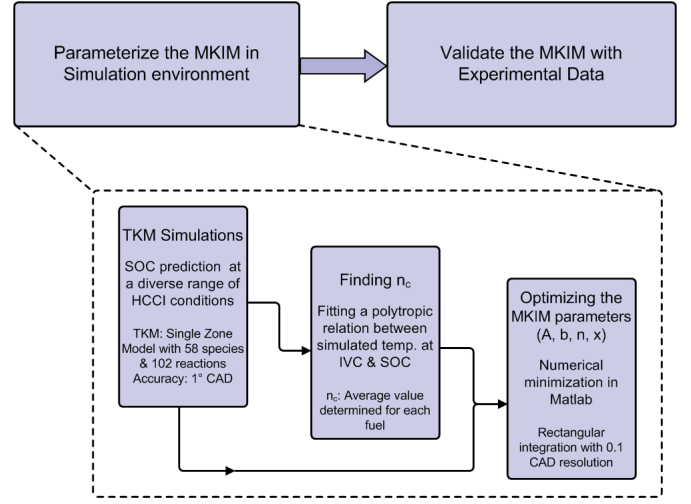


Figure 3: Methodology used to parameterize and validate the MKIM.

blends. The chemical kinetic mechanism is composed of several sub-mechanisms. The ignition, large molecule decomposition, high temperature sub-mechanisms are taken from Zheng et al. [31], with fuel specific rate constants from Li et al [32]. The interaction between the two reference fuels is described using the reaction presented by Tanaka et al [33].

The resulting model which couples together the thermodynamic model with the chemical kinetic mechanism was validated with HCCI experimental data from [34]. The model is calibrated for the single-cylinder engine outlined in Table 3. To calibrate the TKM for the new engine, less than 10% of the experimental points are used. The TKM predicts SOC for the single-cylinder engine with a maximum error of 1 CAD from the range of the experimental data.

Table 3: Configurations of the Ricardo single-cylinder engine.

Parameters	Values
Bore $\times$ Stroke [mm]	80 $\times$ 88.9
Compression Ratio	10
Displacement [L]	0.447
Number of Valves	4
IVC <sup>5</sup> [aBDC]	55°
EVO [aBDC]	-70°

Here, each input is varied independently and simulated with the TKM engine to determine the effects of these engine inputs on the auto-ignition timing. In particular, the engine speed, initial mixture temperature and pressure, EGR percentage<sup>6</sup>, and equivalence ratio are varied over

<sup>5</sup>Valve closing point is defined at the valve lift of 0.15 mm. [30]

<sup>6</sup>EGR(%) is defined as the percent of the total intake mixture which is recycled. [30]

the ranges outlined in Table 4. The input ranges given in Table 4 are chosen to represent typical HCCI operation of the Ricardo single-cylinder engine. TKM simulations are done for the engine using three different blends of two PRFs (N-heptane and iso-octane).

Table 4: Input variations carried out using the TKM

Engine Speed	800, 1000 rpm
IVC Temperature	80, 85,..., 155, 160 °C
EGR(%)	0, 10, 20, 30
Equivalence Ratio	0.5, 0.6, 0.7, 0.8
IVC Pressure	95, 100, 105, 110, 115 kPa
Fuel	PRF0, PRF10, PRF20
Wall temperature	390 °K

From the resulting 8160 simulations, complete combustion occurred in 5131 simulations. Since near-TDC-firing conditions are of the interest, late ignited<sup>7</sup> TKM simulations are excluded. This results in 4752 TKM simulations (Table 5) that are used to estimate the MKIM parameters. The MKIM is only valid for a complete combustion thus only these 4752 simulations are used for parametrization of the MKIM auto-ignition correlation.

Table 5: Number of TKM simulations with an appropriate HCCI combustion

Fuel (PRF)	Engine speed	
	800 rpm	1000 rpm
0	973	907
10	805	735
20	702	630

As Table 5 shows, the number of HCCI auto-ignition points decreases with an increase in engine speed and PRF (octane) number. This is expected as: 1) HCCI combustion is a time-based process and there is less time available when engine speed is increased; and, 2) the chance of auto-ignition increases with a decrease in octane number particularly in this engine with a relatively low compression ratio.

## FINDING THE POLYTROPIC PARAMETER

Using the engine parameter variations for the applied PRF fuels, the values of  $n_c$  can be determined by fitting a polytropic relation between the temperature or pressure at IVC and SOC of the simulations. The value of  $n_c = 1.32$  is chosen using the simulation results of [23].

<sup>7</sup>TKM simulations in which the second stage of HCCI combustion happens at the crank angle higher than 15 degrees after TDC.

## OPTIMIZING THE MKIM PARAMETERS

The parameters of the MKIM equation (6) are fit to minimize the error of the integration, where the target value is 1.0. The numerical minimization is performed using the built-in Matlab function *fminsearch*, which uses the Nelder-Mead simplex minimization method [35]. The integration is carried out numerically with the rectangular method with a step size of 0.1 CAD. The program then uses the optimized parameters and computes the predicted auto-ignition point by integrating (6) until it equals 1.0. The resulting crank angle is taken as the predicted angle of auto-ignition.

## EXPERIMENTAL SETUP

A single cylinder Ricardo Hydra Mark III engine with Rover K7 head is used to carry out HCCI experiments. The geometry of the engine is given in Table 4 and a schematic of the experimental apparatus is shown in Figure 4.

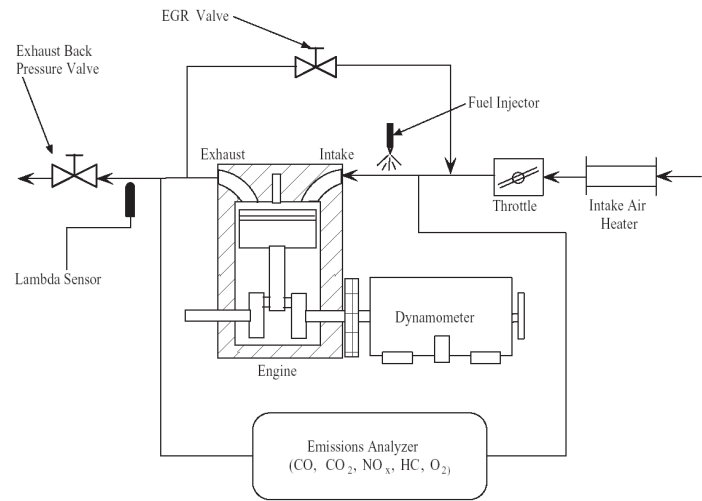


Figure 4: Schematic of the testbench used to obtain experimental data for HCCI validation.

Port fuel injection using a standard automotive fuel injector with 3bar fuel pressure is used. The fuel is injected immediately upstream of the intake valves, and is timed to inject on closed intake valves. The fresh air entering the engine is heated by the electric air heater positioned upstream of the throttle body. Exhaust gas recirculation (EGR) runs through an insulated line from the exhaust to directly after the throttle body in the intake manifold. Intake temperature is measured with a K-type thermocouple positioned in the intake manifold after the mixing of the fresh intake air and EGR, so as to include EGR heating effects. The fresh air heater is operated by a closed-loop controller in order to maintain a constant intake temperature. The recirculated exhaust gas fraction is determined by comparing the CO<sub>2</sub> concentrations in the intake and exhaust manifolds, and by assuming that all CO<sub>2</sub> in the intake manifold is from the exhaust gases. Table 6 shows the engine operating conditions used for experimental val-



idation. IMEP of the engine for these conditions ranges from 4.3 bar to 6 bar. As the compression ratio of the Ricardo engine is only 10, HCCI occurs only for low octane number fuels. PRF20 was the highest PRF blend for which HCCI operation was possible with the Ricardo engine.

Table 6: Engine's operating conditions for HCCI validation.

Engine Speed	800, 1000 rpm
Manifold Temperature	60 - 140 °C
EGR(%)	0% - 28.5%
Equivalence Ratio	0.43 - 0.95
Manifold Pressure	90.5 - 96.3 kPa
Fuel	PRF0, PRF10, PRF20
Coolant Temperature	70 - 80 °C
Oil Temperature	70 - 80 °C

The cylinder pressure is measured with a Kistler water-cooled ThermoCOMP (model 6043A60) piezoelectric pressure sensor that is flush mounted in the cylinder. The manufacturer indicates that the cylinder pressure thermal shock error or short time drift is less than 0.25 bar. The crank angle is measured by a BEI optical encoder with 0.1° resolution connected to the crankshaft on the front of the engine. The cylinder pressure and the encoder signals are measured with an MTS Combustion Analysis System (CAS).

Tests are started by running the engine in part throttle SI mode until the engine reaches operating temperature. The desired intake temperature is then set, and as intake temperatures increase, the throttle is opened and the fueling is manually adjusted to initiate stable HCCI, and to avoid knocking. The EGR rate is adjusted by opening the valve in the EGR line and closing the throttle slightly to pull more exhaust gas into the intake.

For each experimental point, pressure traces from 100 consecutive engine cycles are recorded. Due to amplification of high frequency noise when numerically differentiating the pressure trace to get SOC based on equation (3), the experimental pressure traces are filtered<sup>8</sup>. A fourth order Butterworth low pass filter is used to attenuate the high frequency noise which would have been amplified during differentiation. An experimentally determined cut-off frequency of  $f_c = 0.278\text{CAD}^{-1}$  provides sufficient suppression of high frequency noise, without undue distortion of the pressure trace. As the pressure history was discretized at a constant angular rate (every 0.1CAD), the signal was filtered in the crank angle domain to avoid having to change  $f_c$  for different engine speeds.

<sup>8</sup>To ensure that the auto-ignition timings were indicative of the same phenomena, the same filter was applied on simulated pressure traces.

## RESULTS & DISCUSSION

Using 4752 TKM simulations, the parameters of the MKIM are determined. This process is done for each of the 6 individual cases in Table 5. The estimation process is done in two stages. In the first stage, parameters  $b$ ,  $n$ ,  $x$ , and  $A$  are determined by applying the estimation code on the whole corresponding TKM simulations. Then, the parameter  $A$  is determined for each group of TKM simulations with the same EGR level, keeping the values of  $b$ ,  $n$ , and  $x$  constant from the first stage. Finally, a linear correlation is fit between the  $A$  values and EGR levels.

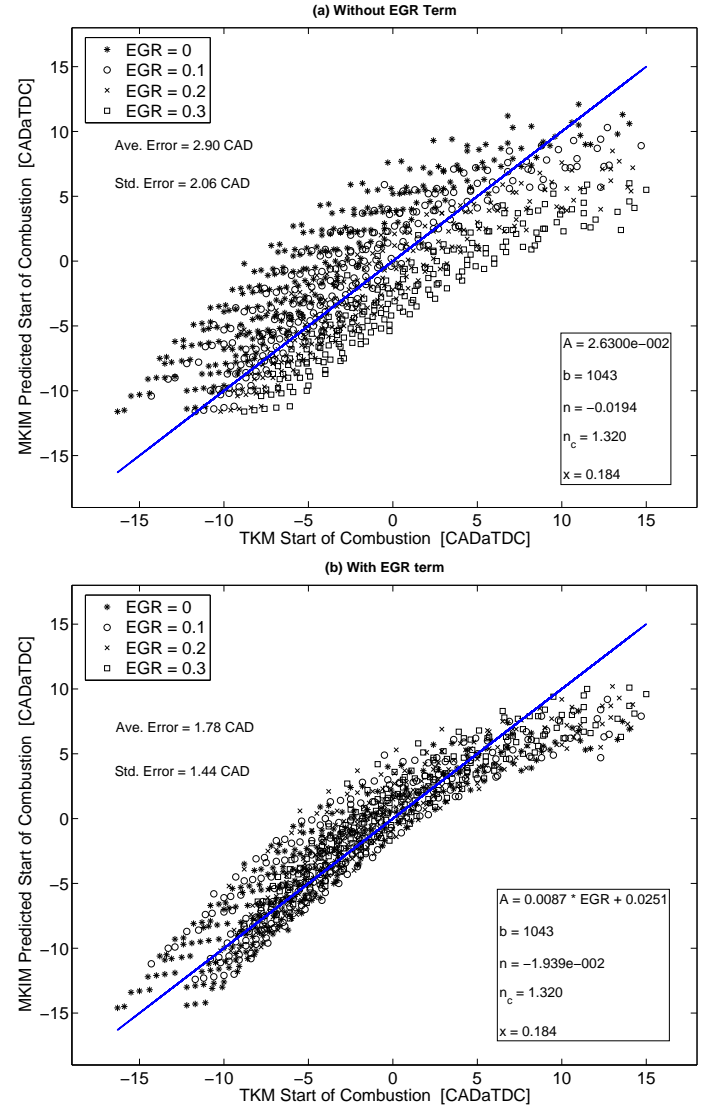


Figure 5: Predicted SOC - main comb. for PRF0 TKM simulations at 800 rpm at various engine conditions using the MKIM. The line represents where the prediction is the same as the actual SOC.

Figure 5 indicates the predicted SOC (for one of 6 cases in Table 5) before (a) and after (b) including the EGR level in the parameter  $A$ . As it can be seen in Figure 5, both average error and standard error are substantially reduced when EGR level is considered in the MKIM. Figure 5 shows the accuracy of the MKIM predictions deteriorates for late auto-ignition. The pre-ignition heating by

the reactions that occur during the large time span prior to the late auto-ignitions probably violates the polytropic assumption used in the MKIM.

The ability of the MKIM to predict the cool flame and main combustion for PRF10 fuel is demonstrated for one case in Figure 6. For the 805 points in the Figure 6, the maximum average error and the maximum standard error for both cool flame and main combustion are 2.09 CAD and 1.57 CAD respectively. The range of average error and standard error for all 6 cases of Table 5 for both cool flame and main combustion cases are 1.48-2.41 CAD and 1.37-2.34 CAD respectively.

Sample values of parameters  $A$ ,  $b$ ,  $n$ ,  $n_c$ , and  $x$  in equation (6) determined for the PRF blends are shown in Figures 5 and 6. The order and sign of these parameters are the same for other cases of Table 5. By examining these parameters it can be seen that for the three PRF blends the SOC advances by increasing the initial temperature and initial pressure, while it retards with an increase in the engine speed. This trend has been also observed in [8]. Furthermore for all three PRF blends studied, SOC happens sooner when equivalence ratio is increased, while SOC is delayed when EGR level is increased. The same trend has been also reported in [3].

The 4752 simulation points, partly shown in Figures 5 and 6, cover a large range of engine inputs (initial temperatures, equivalence ratios, EGR rates, initial pressures, and engine speeds). These results extend previous works [16, 8, 12, 21, 24] on control-oriented modeling of HCCI auto-ignition timing by predicting SOC over a range of engine inputs. However, the model still needs to be cross validated with experimental data which is the subject of the next section.

## EXPERIMENTAL VALIDATION

Experimental data is used to validate the correlation obtained from simulation. Figure 7 compares the predicted SOC with those of experiments for three different fuels at different conditions. In this figure, IVC temperature and pressure are given to the MKIM, so the performance of the IVC correlations presented before is not evaluated. Three different types of information for SOC from the experimental data are indicated in the figure. In Figure 7 two different methods of averaging are used to calculate SOC. In the first method, SOC is calculated from the average pressure trace, while in the second method SOC is calculated by taking the average SOC values from individual cycles for each experiment.

Average error values shown in the figure are the errors between the average SOC from experimental individual cycles (diamond symbols) and the MKIM predicted values (x symbols). There is a good agreement between the SOC of the MKIM and experiment. The total average error for 79 operating points in Figure 7 is 1.7 CAD, while

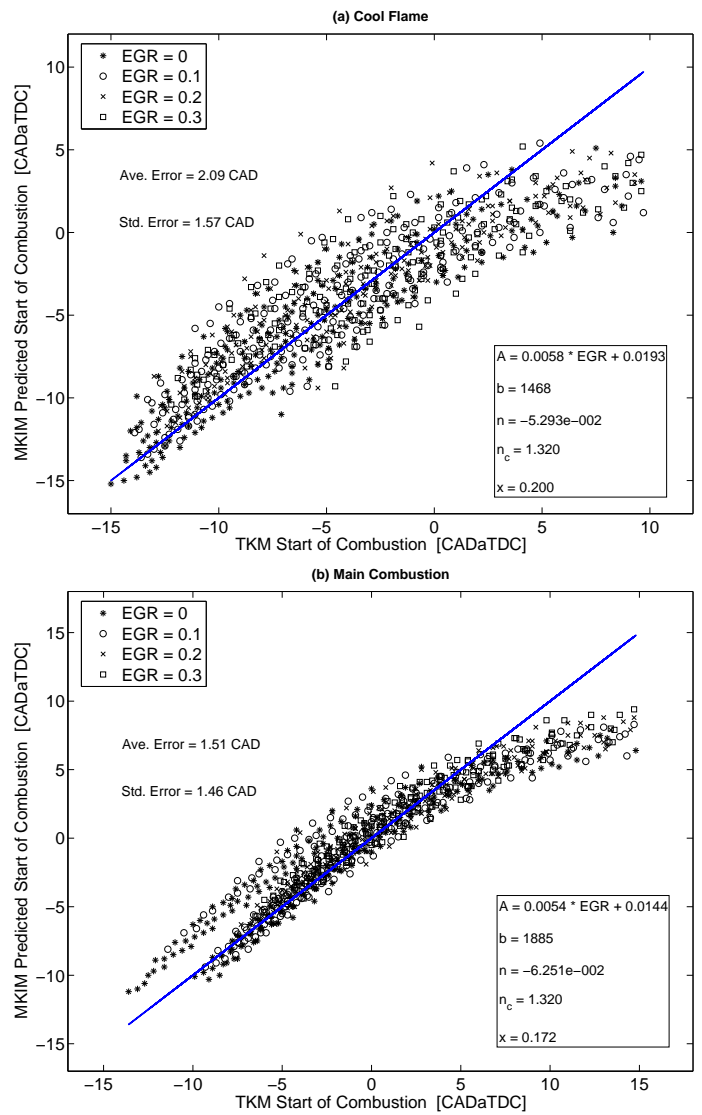


Figure 6: Predicted SOC (a) cool flame and (b) main combustion for PRF10 TKM simulations at various engine conditions at 800 rpm, using the MKIM. The line represents where the prediction is the same as the actual SOC.

the total average error<sup>9</sup> from the range of experimentally calculated SOC is 0.22 CAD. As seen in the figure, the trend of change in SOC from one case to another is captured well for most of the cases. Figure 7 only shows the results for SOC-main combustion since this has more influence on IMEP and heat release. For the cool flame SOC case the error is 2.47 CAD and the total average error is 0.62 CAD. Examining Figure 7 more carefully, it can be seen that a large percentage of the errors comes from the cases with high cyclic variations. The larger the cyclic variation for a case, the larger the error of MKIM prediction. The cyclic variations of HCCI combustion is not captured in the model, and thus cannot be predicted.

Cylinder pressure data are often averaged over recorded cycles to obtain the mean cylinder pressure at each crank

<sup>9</sup>To calculate this term, no error is considered when predicted SOC is within the range of SOC of individual cycles for each experimental point.

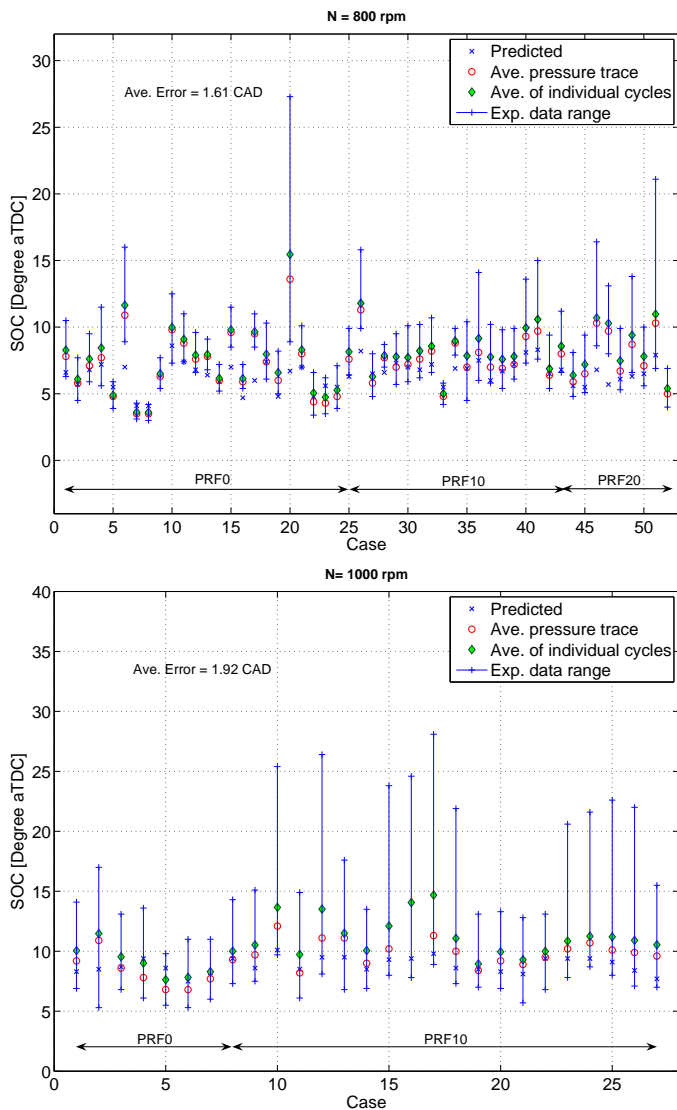


Figure 7: Comparison between predicted and experimental SOC (main comb.) for different PRF blends at various engine conditions, using the MKIM with *IVC* pressure and temperature.

angle. The primary use of this average pressure trace versus crank angle is in calculating the average IMEP which is a linear function of pressure [30]. In some HCCI work [3, 10], this average pressure trace has been used for calculating SOC. This can yield erroneous results, as SOC is not a linear function of the cylinder pressure. The error will become most significant when the combustion cyclic variability is the largest. This can be seen in Figure 7 when the difference between the SOC values from average pressure trace and those averaged on SOC of individual cycles will become larger for the cases with higher cyclic variation. It is best to determine mean SOC by averaging their values obtained from individual cycles.

As seen in Figure 7, some experimental points have a large SOC range while some others have a small range. It also can be observed that SOC variations increase rapidly for late HCCI combustion. The closer the main combustion is to TDC, the more stable it seems to be. Late com-

bustion cycles produce less heat due to quenching that often leads to poor conditions for the next HCCI cycle.

To understand more about the large SOC range for some cases in Figure 7, SOC cyclic variations for two cases from Figure 7 are shown in Figure 8. More engine cycles need to be recorded to capture all different possible patterns of cyclic variations that can happen for each HCCI experimental point (for example in [36] 2800 successive engine cycles are recorded to study HCCI cyclic variations). For some cycles shown in Figure 8, a late combustion is correlated with an early combustion in the next cycle, and vice versa. This can happen because an early auto-ignition timing produces a relatively low in-cylinder pressure and gas temperature at exhaust valve closing. This will cause late combustion of the following cycle that produces a relatively higher cylinder pressure and in-cylinder temperature at exhaust valve closing. This can then trigger an early combustion of the third cycle and so on. Furthermore, a late combustion phasing generates a high level of unburned hydrocarbons in the residuals. These hydrocarbons auto ignite during the following gas exchange phase which can increase the temperature of the residual gases and cause the next combustion cycle to start earlier. [37]

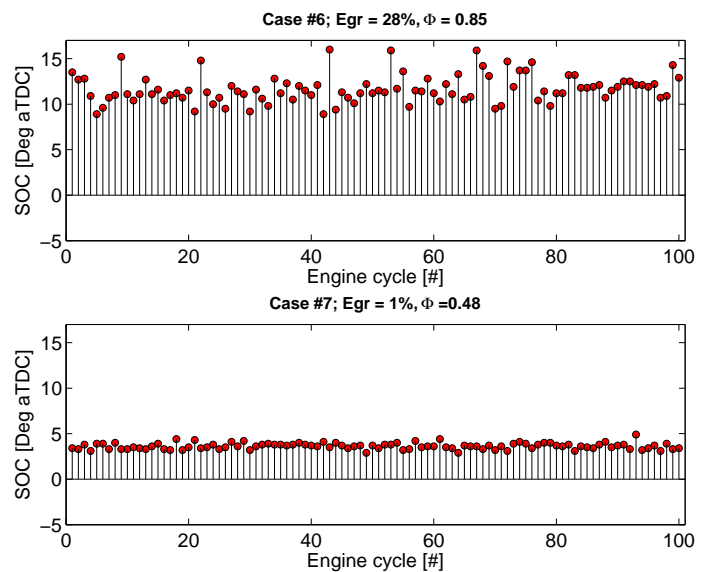


Figure 8: SOC cyclic variations for two sample experimental points in Figure 7 (N800rpm).

However, cyclic variations can also be attributed to the normal variations in equivalence ratio and dilution rate [37] or mixture inhomogeneity [38], providing an explanation for some of the SOC variations in Figure 8.

Figure 9 shows the predicted and experimental SOC for three different fuels when the *IVC* correlations are used. Comparing Figure 7 with Figure 9, the total average error for 79 operating points is increased from 1.7 CAD to 1.99 CAD and the total average error from the range of experimentally calculated SOC is increased from 0.22 CAD to 0.39 CAD. For cool flame predictions, the total average

error is increased from 2.47 CAD to 2.62 CAD, while the total average error from the range of experimentally calculated SOC is increased from 0.6 CAD to 0.77 CAD. This increased error is caused by the inherit error of equation (1) and (2) and the influence of initial temperature and pressure on SOC. If measured manifold values are used instead of the values from IVC correlations, the total average error for the main combustion and cool flame become 7.4 CAD and 8.7 CAD respectively and the total average error from the range of experimentally calculated SOC for main combustion and cool flame become 4.5 CAD and 6.3 CAD respectively.

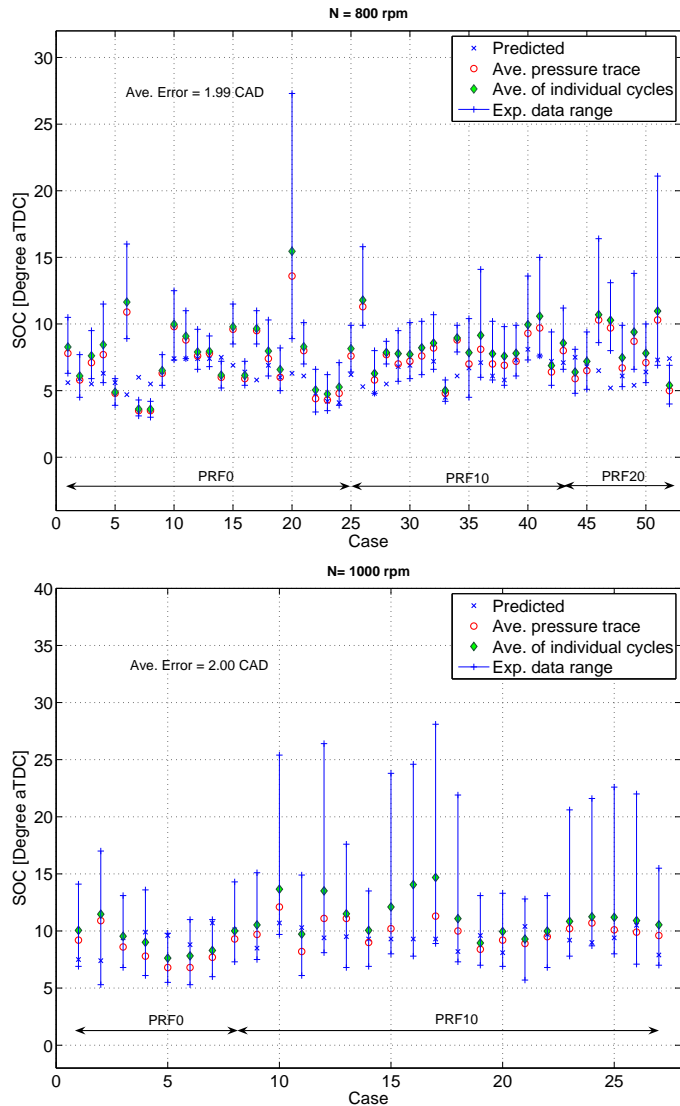


Figure 9: Comparison between predicted and experimental SOC (main comb.) for three PRF blends at various engine conditions, using the MKIM with *intake manifold* pressure and temperature.

The agreement between the SOC of the MKIM and experiment is good particularly since the MKIM was parameterized using the TKM simulation and then validated with experimental data. The parameters of the MKIM are estimated using TKM simulations not directly with experimental data. Since the TKM does not exactly represent the real engine more variation to experiment is expected. One

possible way to avoid this is to have more extensive measurement data from the engine; however, this will increase the cost.

## CONCLUSIONS

A Modified Knock Integral Model (MKIM) was extended to become suitable for real-time applications for HCCI engines. Two simple correlations were introduced to relate measured temperature and pressure of the intake manifold to their values at IVC. TKM simulation results are used to parameterize the MKIM which is validated with HCCI experimental points (none of which are used to parameterize the MKIM). The resulting model doesn't require any instantaneous in-cylinder parameters but only needs intake manifold temperature and pressure, EGR rate, and equivalence ratio to predict auto-ignition timing. The developed MKIM can be used not only to predict the start of the main combustion but also to predict the start of the cool flame.

The presented model was cross validated for a large number of TKM simulations (4752 points) and HCCI experiments (79 points). This extends our previous validation of the MKIM showing good model prediction for different engine inputs. The MKIM is able to predict auto-ignition timing for the experimental HCCI engine with an average error of less than 2 CAD. However, the MKIM becomes less accurate for very late auto-ignition timing because in these cases the polytropic assumption of compression is violated with pre-ignition heating from the reactions that happen during the large time span before auto-ignition.

For an HCCI engine cyclic variations of SOC are typically low but can increase when HCCI auto-ignition occurs late. To accurately predict SOC for these HCCI operating points, the simulation model should consider this phenomenon and must be extended.

A proper method of averaging is required to calculate SOC from the cycle by cycle recorded in-cylinder pressure data. As SOC is not linearly related to the cylinder pressure, erroneous SOC is calculated by using the average pressure trace for HCCI experiments with combustion variability. It is best to determine mean SOC by averaging their values obtained from individual cycles.

## FUTURE WORK

Although the start of combustion is successfully predicted by the correlation presented in this paper, there are many other issues to be investigated. The performance of the model needs to be evaluated for the fuels with higher PRF blends than used in this study. As TKM may not be always available, a methodology to parameterize the MKIM with the minimum required HCCI experiments is needed. Furthermore, to evaluate the MKIM for controlling the SOC of an HCCI engine, the MKIM should be converted to a realtime open loop scheduling of engine variables on a

real engine. The possible scheduled engine variables can be intake temperature (heater), intake pressure (supercharger), EGR level (electronic valve), and fuel type (fuel modulating system).

To account for high cyclic variations for some HCCI conditions, a more detailed study of SOC variations of HCCI engines is required. The results of this study can be used to extend the MKIM to include the HCCI cyclic variations as well. For complete control of HCCI combustion, in addition to SOC, combustion phasing (CA50<sup>10</sup>) and combustion duration should be controlled. The MKIM can be developed to be used in conjunction with other models to predict combustion phasing and combustion duration.

## REFERENCES

- [1] F. Zhao, T. W. Asmus, D. N. Assanis, J. E. Dec, J. A. Eng, and P. M. Najt. "Homogeneous Charge Compression Ignition (HCCI) Engines". SAE Publication PT-94, 2003.
- [2] R. H. Stanglmaier and C. E. Roberts. "Homogeneous Charge Compression Ignition (HCCI): Benefits, Compromises, and Future Engine Applications". SAE Paper No. 1999-01-3682, 1999.
- [3] X. Lü, W. Chen, Y. Hou, and Huang Z. "Study on the Ignition, Combustion and Emissions of HCCI Combustion Engines Fueled With Primary Reference Fuels". SAE Paper No. 2005-01-0155, 2005.
- [4] S. C. Kong and R. D. Reitz. "Numerical study of premixed HCCI engine combustion and its sensitivity to computational mesh and model uncertainties". *Combustion Theory and Modeling*, pages 417–433, 2003.
- [5] M. Embouazza, D. C. Haworth, and N. Darabiha. "Implementation of Detailed Chemical Mechanisms into Multidimensional CFD Using in situ Adaptive Tabulation: Application to HCCI Engines". SAE Paper No. 2002-01-2773, 2002.
- [6] N. P. Komninou, D. T. Hountalas, and D. A. Kouremenos. "Description of in-Cylinder Combustion Processes in HCCI Engines Using a Multi-Zone Model". SAE Paper No. 2005-01-0171, 2005.
- [7] D. L. Flowers, S. M. Aceves, J. Martinez-Frias, and R. W. Dibble. "Prediction of carbon monoxide and hydrocarbon emissions in iso-octane HCCI engine combustion using multizone simulations". *Proceedings of the Combustion Institute*, pages 687–694, 2002.
- [8] J. Bengtsson, M. Gafvert, and P. Strandh. "Modeling of HCCI Engine Combustion for Control Analysis". pages 1682–1687. IEEE conference on decision and control, 2004.
- [9] M. Roelle, G. M. Shaver, and J. C. Gerdes. "Tackling the Transition: A Multi-Mode Combustion Model of SI and HCCI for Mode Transition Control". pages 329–336. ASME International Mechanical Engineering Congress, 2004.
- [10] S. Karagiorgis, N. Collings, K. Glover, and T. Petridis. "Dynamic Modeling of Combustion and Gas Exchange Processes for Controlled Auto-Ignition Engines". *Proceeding of the 2006 American Control Conference*, Minneapolis, Minnesota, USA, June 14–16, 2006.
- [11] M. Canova, L. Garzarella, M. Ghisolfi, Mohler S. M., Guezennec Y., and Rizzoni G. "A control-oriented mean-value model for HCCI diesel engines with external mixture formation". *Proceedings of IMECE2005*, ASME International Mechanical Engineering Congress, 2005.
- [12] G. M. Shaver, J. C. Gerdes, J. Parag, P. A. Caton, and C. F. Edwards. "Modeling for Control of HCCI Engines". pages 749–754. American Control Conference, 2003.
- [13] M. Halstead, L. Kirsch, and J. Keck. "The autoignition of hydrocarbon fuels at high temperatures and pressures-fitting of a mathematical model". volume 30, pages 45–60. *Combustion and Flame*, 1977.
- [14] G. M. Shaver, M. Roelle, and Gerdes J. C. "Tackling the Transition: Decoupled Control of Combustion Timing and Work Output in Residual-Affected HCCI Engines". pages 3871–3876. American Control Conference, 2005.
- [15] Stephen R. Turns. *An Introduction to Combustion: Concepts and Applications*. McGraw-Hill, 2nd edition, 2000.
- [16] D. J. Rausen, A. G. Stefanopoulou, J-M. Kang, J. A. Eng, and W. Kuo. "A Mean-Value Model for Control of Homogeneous Charge Compression Ignition (HCCI) Engines". pages 125–131. American Control Conference, 2004.
- [17] C. J. Chiang and A. G. Stefanopoulou. "Sensitivity Analysis of Combustion Timing and Duration of Homogeneous Charge Compression Ignition (HCCI) Engines". *Proceeding of the 2006 American Control Conference*, Minneapolis, Minnesota, USA, June 14–16, 2006.
- [18] J. C. Livengood and P. C. Wu. "Correlation of Autoignition Phenomena in Internal Combustion Engines and Rapid Compression Machines". pages 347–356. Fifth Symposium (International) on Combustion, 1955.
- [19] F. Agrell, H. E. Ångström, B. Eriksson, J. Wikander, and J. Linderyd. "Integrated Simulation and Engine Test of Closed Loop HCCI Control by Aid of Variable Valve Timings". SAE Paper No. 2003-01-0748, 2003.

<sup>10</sup>The crank angle by which 50% of the fuel has been burnt.

- [20] Y. Ohyama. "Engine Control Using a Real-Time Combustion Model". SAE paper No. 2001-01-0256, 2001.
- [21] J. S. Souder, P. Mehresh, J. K. Hedrick, and R. W. Dibble. "A Multi-Cylinder HCCI Engine Model for Control". pages 307–316. ASME International Mechanical Engineering Congress, 2004.
- [22] M. Iida, T. Aroonsrisopon, M. Hayashi, D. Foster, and J. Martin. "The Effect of Intake Air Temperature, Compression Ratio and Coolant Temperature on the Start of Heat Release in an HCCI Engine". SAE Paper No. 2001-01-1880, 2001.
- [23] K. Swan, M. Shahbakhti, and C. R. Koch. "Predicting Start of Combustion Using a Modified Knock Integral Method for an HCCI Engine". SAE Paper No. 2006-01-1086, 2006.
- [24] Y. Ohyama. "Engine Control Using Combustion Model". SAE paper No. 2000-01-0198, 2000.
- [25] P. Kirchen, M. Shahbakhti, and C. R. Koch. "A Skeletal Kinetic Mechanism for PRF Combustion in HCCI Engines". *Journal of Combustion Science and Technology*, Accepted and will be published in future volumes, 2007.
- [26] S. Tanaka, F. Ayala, J. C. Keck, and J. B. Heywood. "Two-stage Ignition in HCCI Combustion and HCCI Control by Fuels and Additives". *Journal of Combustion and Flame*, Vol. 132, p. 219-239, 2003.
- [27] M. D. Checkel and J. D. Dale. "Computerized Knock Detection From Engine Pressure Records". SAE Paper No. 860028, 1986.
- [28] G. M. Rassweiler and L. Withrow. "Motion Pictures of Engine Flames Correlated with Pressure Cards". *SAE*, 42:185–204, 1938.
- [29] T. Noda, K. Hasegawa, M. Kubo, and T. Itoh. "Development of transient knock prediction technique by using a zero-dimensional knocking simulation with chemical kinetics". SAE Paper No. 2004-01-0618, 2004.
- [30] J. B. Heywood. *Internal Combustion Engine Fundamentals*. McGraw-Hill, 1988.
- [31] J. Zheng, W. Yang, D. L. Miller, and N. P. Cernansky. "A skeletal chemical kinetic model for the HCCI combustion process". SAE Paper No. 2002-01-0423, 2002.
- [32] H. Li, D. L. Miller, and N. P. Cernansky. "Development of a reduced chemical kinetic model for prediction of preignition reactivity and autoignition of primary reference fuels". SAE Paper No. 960498, 1996.
- [33] S. Tanaka, F. Ayala, and J. C. Keck. "A Reduced chemical kinetic model for HCCI combustion of primary reference fuels in a rapid compression machine". *Combustion and Flame*, 133:467–481, 2003.
- [34] M. J. Atkins and C. R. Koch. "The Effect of Fuel Octane and Diluent on HCCI Combustion". *Proceeding of IMechE - Part D*, 219:665 – 675, 2005.
- [35] J. A. Nelder and R. Mead. "A Simplex Method for Function Minimization". *Computer Journal*, pages 308–313, 1965.
- [36] R. M. Wagner, K. D. Edwards, C. S. Daw, J. B. Green Jr., and B. G. Bunting. "On the Nature of Cyclic Dispersion in Spark Assisted HCCI Combustion". SAE Paper No. 2006-01-0418, 2006.
- [37] L. Koopmans, O. Backlund, and I. Denbratt. "Cycle to Cycle Variations: Their Influence on Cycle Resolved Gas Temperature and Unburned Hydrocarbons from a Camless Gasoline Compression Ignition Engine". SAE Paper No. 2002-01-0110, 2002.
- [38] S. Yamaoka, H. Kakuya, S. Nakagawa, Toshiharu Nogi, A. Shimada, and Y. Kihara. "A Study of Controlling the Auto-Ignition and Combustion in a Gasoline HCCI Engine". SAE Paper No. 2004-01-0942, 2004.

## ABBREVIATIONS

aBDC:	after Bottom Dead Center
AFR:	Air Fuel Ratio
CAD:	Crank Angle Degree
CFD:	Computational Fluid Dynamics
CO <sub>2</sub> :	Carbon Dioxide
dp3Lim:	Threshold Limit for 3 <sup>rd</sup> Derivative of Pressure Trace
EGR:	Exhaust Gas Recirculation
EVO:	Exhaust Valve Opening
HCCI:	Homogeneous Charge Compression Ignition
IMEP:	Indicated Mean Effective Pressure
IVC:	Intake Valve Closing
KIM:	Knock Integral Model
MKIM:	Modified Knock Integral Model
NTC:	Negative Temperature Coefficient
PRF:	Primary Reference Fuels
RPM:	Revolution per Minute
SI:	Spark Ignition
SOC:	Start of Combustion
TDC:	Top Dead Center
TKM:	Thermo-Kinetic Model